(2)

ARVIN/CALSPAN

AD-A161 753

A CHAMBER INVESTIGATION OF THE IR AND VISIBLE WAVELENGTH OBSCURATION PROPERTIES OF PYROTECHNICALLY GENERATED SMOKES

BY

J.T. Hanley and E.J. Mack

May 1985

Calspan Report No. 7278-1
Contract No. N00014-84-C-2174

Prepared for:

NAVAL RESEARCH LABORATORY
4555 Overlook Avenue, S.W.
Washington, D.C. 20375
CODE: 4110

CALSPAN CORPORATION P.O. BOX 400 BUFFALO, NEW YORK 14225

TABLE OF CONTENTS

LIST OF FIGURES

LIST OF TABLES

Section 1

INTRODUCTION AND SUMMARY OF RESULTS

Background

Under Contract No. N00014-84-C-2174 with the Naval Research Laboratory, Calspan Corporation continued its laboratory evaluation of hygroscopic pyrotechnic smoke screens, a collaborative investigation with several Navy laboratories now in its seventh year.* The overall objective of the program is the development of an effective screening agent to both visible and IR wavelengths utilizing pyrotechnically-generated hygroscopic aerosol. Calspan's primary role in the Navy program is to evaluate the extinction performance of pyrotechnics developed by the Naval Weapons Center and to provide recommendations directed at improving the extinction performance of these smokes. The evaluation is conducted in Calspan's 600 m^3 test chamber and includes measurement of the smokes' mass extinction coefficient, yield factors, chemical composition and particle size distribution.

In general, the NWC pyrotechnics are formulated to produce smokes of alkali-halide salt particles upon combustion. The primary advantage of such pyrotechnics is their ability to produce copious numbers of hygroscopic aerosol, which, when exposed to a sufficient level of ambient humidity, deliquesce to form solution droplets of approximately twice their original size and five times their original mass. Thus, only a fraction of the resultant cloud mass (smoke screen) originates from the pyrotechnic, the remaining mass being supplied by atmospheric water vapor.

Objectives of Current Program

In pursuit of an effective IR wavelength screen and an increased understanding of the particle formation mechanisms and resultant size distribution,

---

* The first four years of the investigation were conducted under the sponsorship of the Naval Air Systems Command, AIR 32R (formerly AIR 310C).

the primary objective of this year's effort was to evaluate the influence of an energetic binder (GAP) on the performance of two pyrotechnics, one which produced a KCl aerosol, the other a mixed aerosol of $MgCl_2$ and carbon. Comparison tests were run, in Calspan's 600 m^3 test chamber, in which the performance of the energetic vs. non-energetic pyrotechnics was compared in terms of mass yield, payload mass extinction coefficient, aerosol decay rate and size distribution.

A secondary objective of limited scope was to investigate the potential of using IR absorbing surface active agents to coat the smoke aerosol so as to enhance the smoke's IR wavelength absorption as well as inhibit subsequent aerosol evaporation upon exposure to decreasing humidity.

Summary of Major Results

Perhaps the most significant finding resulting from this year's effort involves the influence of the energetic binder on the performance of the carbonous smoke producing LM14 pyrotechnic. As a result of using an energetic binder (GAP), the LM14 pyrotechnic has a nominal mass yield averaging 72% as compared to ~40% for its non-energetic counterpart LM13 and the 25-40% yields typical of the earlier NWC pyrotechnics. Additionally, the use of the energetic binder resulted in a shift of the size distribution of the carbonous LM14 smoke aerosol to smaller sizes, effecting a significant reduction in the aerosol fall out rate relative to the non-energetic LM13. As a result of the increased yield and reduced aerosol decay rate, the LM14 pyrotechnic provides the best overall performance (based on combined IR and visible wavelength extinction and aerosol decay rate) of the NWC pyrotechnics evaluated on this program.

A limited study on the use of surface active agents to provide enhanced IR absorption and inhibit droplet evaporation has defined several organic polymers which appear to have the potential to form hard, non-volatile skins on deliquesced aerosol. Further development of laboratory screening tests is needed to confirm and quantify these preliminary results.

The above topics are discussed in greater detail within the body of this report. Section 2 describes the chamber facility, instrumentation and test procedures. Results of the chamber evaluation of the extinction characteristics of the NWC pyrotechnics are presented in Section 3. Section 4 presents the results of the investigation into the use of surface active agents to enhance IR absorption and inhibit droplet evaporation. Section 5 summarizes the principal conclusions from this year's effort and presents recommendations for further areas of investigation.

Definition of extinction and yield parameters is provided in Appendix A. Appendix B presents time-history plots of extinction and aerosol mass loading during the chamber tests of the NWC pyrotechnics.

Section 2

FACILITIES AND PROCEDURES

2.1 Facilities and Instrumentation

The Calspan chamber is cylindrical with a diameter and height of 9.1 meters enclosing a volume of 590 m^3. The inner chamber surface is coated with a fluoroepoxy type urethane (developed at the Naval Research Laboratory, Washington, DC) which has surface energy and reactivity properties comparable to those of the FEP Teflon. A complete air handling capability permits the removal of virtually all particulate and gaseous contaminants prior to each experiment, the introduction of specified aerosols, and control of humidity from 30 to 97% RH. Figure 1 presents an interior view of the chamber.

Instrumentation used during the present program to monitor aerosol behavior within the chamber included visible and IR wavelength transmissometers, a 6 stage Batelle cascade impactor and a quantitative filtration system for determination of aerosol mass loading. Specific details of the instrumentation and chamber facility may be found in prior report (References 1-6).

Extinction of electromagnetic radiation by the pyrotechnic smokes was measured at visible wavelength over a path of ~2 m. A lense collimated beam from an incandescent bulb powered by a regulated power supply was focused on an RCA 4440 photomultiplier detector. The photomultiplier has a peak sensitivity in the range 0.4-0.5 um wavelength.

The IR transmissometer utilizes an 18.3 m path length, a 900°C black body source, and an HgCdTe detector operated at liquid nitrogen temperature. The source beam, chopped and collimated, is directed through the chamber (at a height of 1.5 m) and folded back to the detector by spherical front silvered mirrors. Continuous measurements of extinction as a function of wavelength are obtained via a variable wavelength filter wheel located in front of the detector. The spectral resolution of this filter is two percent over the wavelength interval from 2.5-14 um. Data acquisition and reduction are computer controlled. Intensity measurements are obtained at approximately 0.02 um wavelength intervals, with a complete 2.5-14 um scan requiring 2 minutes.

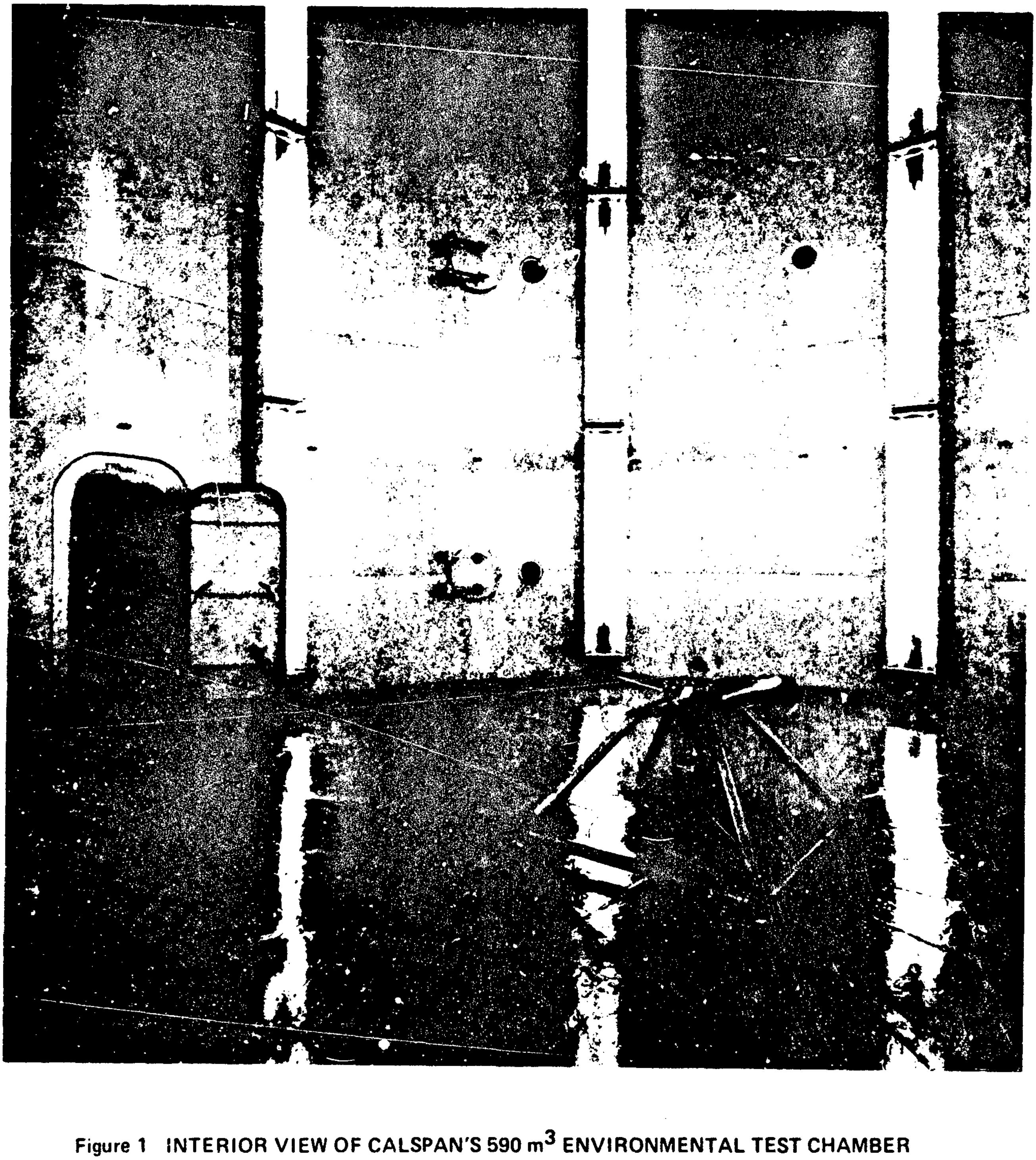

Figure 1 INTERIOR VIEW OF CALSPAN'S 590 m^3 ENVIRONMENTAL TEST CHAMBER

2.2 Generation of Pyrotechnic Smokes in the Chamber Tests

Prior to each test, the chamber was filtered of background aerosol and brought to the desired relative humidity. A preweighed quantity of the pyrotechnic was then ignited within the chamber using either a propane torch or a remote, hot wire ignition system. After allowing five minutes for the smoke to become uniformly mixed and for the hygroscopic aerosol to come to equilibrium at the chamber humidity, measurements were made of appropriate parameters. The smokes were continuously stirred to insure homogeneous conditions throughout the chamber during each test.

2.3 Mass Loading Samples

Mass loading aerosol samples were drawn upon Pallflex type QAOT quartz fiber filters. Sampling duration was typically fifteen minutes at a nominal rate of 1 cfm. Sample flow rate was controlled by use of a calibrated 1 cfm critical orifice with appropriate flow correction for upstream vacuum. To assure the attainment and maintenance of critical flow through the orifice, both upstream and downstream vacuums were monitored. Additionally, a flowmeter was placed in the sampling line providing a direct visual check of the flow rate.

Assessment of aerosol mass loading within the chamber involved the acquisition of several filter samples as follows: after bringing the chamber to the desired test humidity, a duplicate pair of background filter samples was drawn to assess the mass change due to the inherent hygroscopicity of the filter material. Upon completion of the background sampling, the pyrotechnic was ignited. After waiting five minutes for the aerosol to become uniformly mixed throughout the chamber, a series of duplicate mass loading samples were obtained. Duplicate samples (run side by side, simultaneously) were obtained to add confidence to the mass loading values. During the tests, up to four pairs of duplicate samples were drawn sequentially to assess the rate of aerosol mass decay.

Due to the hygroscopicity of the smoke samples, the filters were weighed directly within the chamber environment immediately after sampling. In this way, errors caused by condensation upon or evaporation from the hygroscopic samples due to exposure to humidities different from those of the test humidity were avoided.

To assess the nominal aerosol mass loading, the filter samples were removed from the chamber, baked at 110°C for one hour to remove all condensed water, and reweighed.

SECTION 3

THE CHAMBER EVALUATION OF THE EXTINCTION AND AEROSOL CHARACTERISTICS OF THE NWC PYROTECHNICS

3.1 Log of Experiments

Table 1 presents a log of the chamber tests performed on the current program. For each test, the pyrotechnic payload and chamber relative humidity are presented along with the type of data obtained. These data include visible and IR wavelength extinction measurements, yield factors and cloud mass decay rates obtained from mass loading filter samples, size distribution data derived from cascade impactor measurements and the acquisition of filter samples for examination via electron microscopy.

In all, 13 tests were performed. The primary tests involved 80 g payloads of each of the new NWC pyrotechnics (LM 13, 14, 15 and 16) at high and low humidity, tests 1 through 4 and 5 through 8, respectively. Tests 9 through 11 were conducted to verify and complement the results obtained during tests 1 and 2. Due to the limited quantity of pyrotechnic available for testing, tests 9 through 11 were conducted with 10 g payloads. In tests 12 and 13, payloads of munition grade white phosphorus felt wedges were used for comparison to the NWC pyrotechnics and to pure laboratory grade white phosphorus used in previous years.

3.2 The Chemical Composition of the NWC Pyrotechnics and Their Resultant Smokes

Table 2 presents the chemical composition of the LM 13, 14, 15 and 16 pyrotechnics and their resultant smokes. These data were provided by NWC (Dr. L. Mathews and Dr. C. Dinerman) with the smoke compositions being derived from NWC's thermochemistry computer program. Also included in the table is the density of the pyrotechnics as measured at Calspan using standard water displacement/gravimetric techniques.

Table 1
LOG OF CHAMBER TESTS CONDUCTED DURING FY84

TEST PARAMETERS				DATA OBTAINED (X)					
TEST NO.	PAYLOAD		RH	EXTINCTION		MASS YIELD	MASS DECAY	SIZE DIST.	SEM FILTER
				VIS	IR				
1	80g	LM13	89%	–	X	X	X		
2	80g	LM14	88%	X	X	X	X		
3	80g	LM15	89%	X	X	X	X		
4	80g	LM16	88%	X	X	X	X		
5	80g	LM13	40%	X	X	X	X	X	X
6	80g	LM14	39%	X	X	X	X	X	X
7	80g	LM15	40%	X	X	X	X	X	X
8	80g	LM16	39%	X	X	X	X	X	X
9	10g	LM13	89%	–	X	–			
10	10g	LM13	76%	X	X	X			
11	10g	LM14	76%	X	–	X			
12	23.5g	WP WEDGE	79%	X	X	X			
13	6.1g	WP WEDGE	39%	X	X	X			

Table 2

CHEMICAL COMPOSITION OF THE NWC PYROTECHNICS AND THEIR ASSOCIATED SMOKES (PROVIDED BY NWC)

	PYROTECHNIC COMPOSITION (WEIGHT PERCENT)		SMOKE COMPOSITION (WEIGHT PERCENT)	
LM13	HYDROCARBON BINDER	32%	CARBON	35%
	MAGNESIUM	14%	MgO	2%
	HEXACHLOROBENZENE	54%	$MgCl_2$	54%
			HCl	3%
	BULK DENSITY = 1.4 g/cm^3		H_2	3%
			CO	3%
LM14	ENERGETIC BINDER (GAP)	32%	CARBON	21%
	MAGNESIUM	14%	$MgCl_2$	55%
	HEXACHLOROBENZENE	54%	Mg	1%
			HCl	2%
	BULK DENSITY = 0.87 g/cm^3		H_2	1%
			CO	8%
			N_2	11%
LM15	HYDROCARBON BINDER	25%	MgO	7%
	MAGNESIUM	5%	Mg	1%
	POTASSIUM PERCHLORATE	70%	KCl	40%
			CO	32%
	BULK DENSITY = 1.7 g/cm^3		CO_2	10%
			H_2O	9%
			H_2	1%
LM16	ENERGETIC BINDER (GAP)	25%	KCl	40%
	MAGNESIUM	5%	MgO	8%
	POTASSIUM PERCHLORATE	70%	O_2	10%
			NO	1%
	BULK DENSITY = 2.0 g/cm^3		CO_2	19%
			H_2	<1%
			H_2O	7%
			CO	5%
			N_2	8%

The pyrotechnics were formulated so that the influence of energetic binders on pyrotechnic performance, particularly yield and particle size, could be assessed. Thus, the LM 13 and 14 pyrotechnics differ only in that LM14 uses an energetic binder (GAP) whereas LM13 uses a non-energetic hydrocarbon binder. Both the LM 13 and 14 pyrotechnics generate a $MgCl_2$/Carbon smoke. Likewise, the LM 15 and 16 pyrotechnics differ only in that LM16 uses the energetic binder. Both the LM15 and 16 pyrotechnics generate a KCl smoke aerosol.

Upon receipt of the NWC pyrotechnics for testing, it was apparent that significant density differences existed between the different formulations. As shown in Table 2, the pyrotechnic densities ranged from 0.87 to 2.0 g/cm^3 for LM14 and LM16 respectively. While pyrotechnic density is not a factor in determining the usual mass normalized extinction and efficiency factors, in actual field deployment, payload volume is often more important than payload mass. Thus, all other factors being equal, high density formulations are preferred.

3.3 Payload Mass Extinction Coefficient (αp)

Before presenting results on the payload mass extinction coefficient, hereafter referred to as αp, it is beneficial to discuss how α p and cloud mass loading vary with time during the chamber tests due to both particle fallout and coagulation.

- The decay of cloud mass and extinction during the chamber tests.

As was noted in a previous series of chamber tests with the LM 11 and 12 pyrotechnics (Hanley et. al., 1983), these smokes, which were composed of $MgCl_2$ and carbon similar to the smokes of the current LM 13 and 14 pyrotechnics, had significantly greater decay rates of cloud mass and extinction than the non-carbonous NaCl-KCl smokes generated by, for example, the CY85A pyrotechnic and the current LM 15 and 16 pyrotechnics. The greater decay rate of the carbonous smokes is attributed to the relatively large size of the carbon particles ($\sim$10 μm diam.) found in these smokes.

The impact of cloud decay on the utility of the pyrotechnics is directly dependent upon the desired duration of smoke coverage. If only relatively short time periods are involved, say less than $\sim$10 minutes, then a relatively rapid

decay rate can be tolerated. However, if smoke coverage is required for longer periods, of up to several hours or longer as has been discussed in some deployment concepts for the NWC smokes, then decay rates must be kept at a minimum.

In response to the observed decay of the carbonous smokes, an effort was made during this year's tests to quantify the decay of cloud mass and extinction during the ∿60 minute period following smoke generation. Thus, during tests 1 through 8, continuous measurements were made of visible and IR wavelength extinction and a sequential series of mass loading filter samples was drawn so that the decay of cloud extinction and mass could be quantified.

As an example of cloud decay, Figure 2 shows the time history of cloud mass loading and IR extinction in the 3-5 μm and 8-12 μm band which occurred during test 1 for the carbonous LM13 smoke at high humidity. This particular test had the greatest decay observed during the test series. As can be seen, after approximately 20 minutes, α_p at 8-12 μm was reduced by 50% of its initial value with an approximate 35% reduction in the 3-5 μm band and a 30% reduction in cloud mass. The more rapid decay of α_p in the 8-12 μm band is apparently due to the strong dependence of extinction in this wavelength band on large particle scattering and the relatively rapid fallout of these larger particles. As will be discussed later in this section, the use of an energetic binder in the LM14 pyrotechnic resulted in a substantial decrease in the decay rate of the carbonous smoke relative to that for the non-energetic LM13 shown in Figure 2.

(In contrast to the significant decay which occurred for the carbonous smoke during test 1 discussed above, the KCl smokes (e.g., tests 3 and 4 as presented in Appendix B) showed only slight decay of cloud mass and visible wavelength α_p. Furthermore, at the 3-5 μm and 8-12 μm IR bands, slow increases in α_p were observed with time for these smokes. Such increases apparently result from small-particle coagulation leading to a gradual increase in particle scattering at longer wavelengths, though the possibility of humidity drift and/or optics contamination by the smoke cannot, at present, be entirely ruled out.)

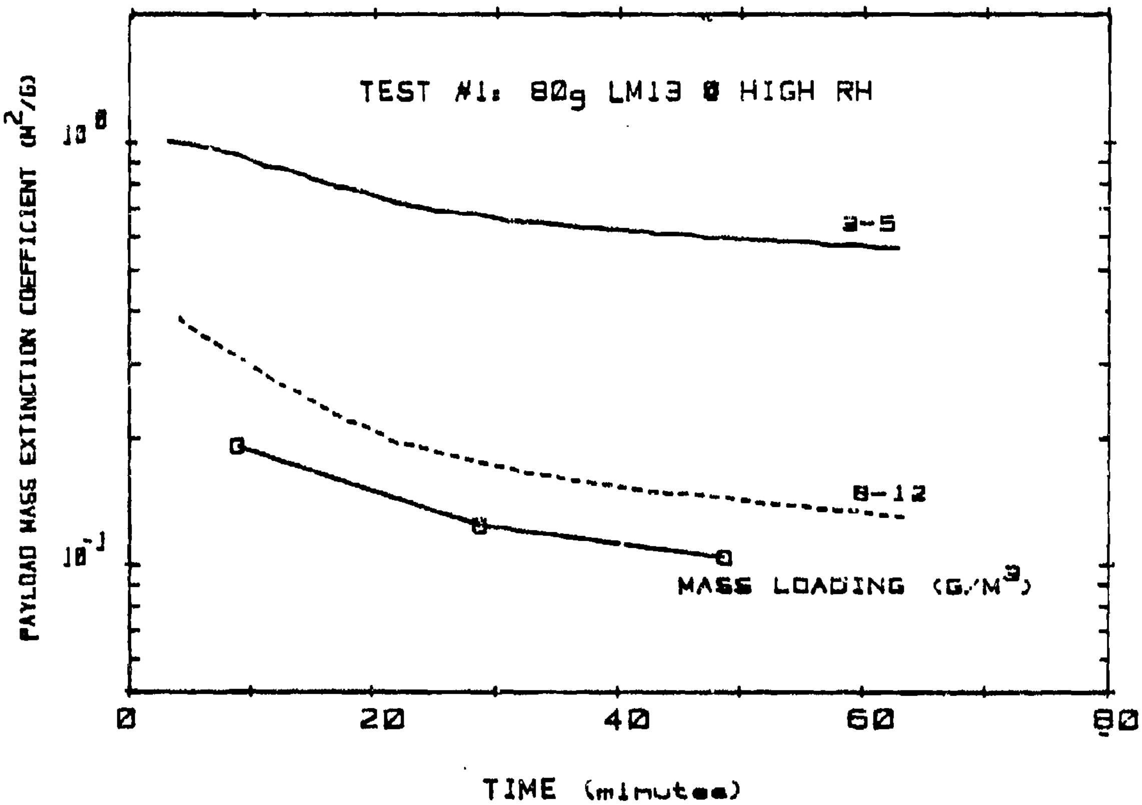

Figure 2. Example of smoke mass loading and extinction decay: Test 1, LM13 @ high humidity. This particular test had the greatest decay observed during the test series.

The decay of cloud mass and extinction adds a complication to the analysis and interpretation of the test data since values of αp and cloud mass are time dependent. Standard practice when dealing with decaying cloud systems in chamber tests is to report values extrapolated back to "time zero" - the time at which the smoke was first generated. Thus, the extinction and yield data presented below for the NWC pyrotechnics are reported at time zero as extrapolated directly from the time history plots presented in Appendix B. Additionally, the decay rates of these parameters, in terms of their half life, are also presented. As seen in Figure 2, the decay rate of extinction and mass loading was not constant, with the greatest decay occurring at the beginning of the test. To adequately define this period of the most significant decay, the half-life values reported are based on approximately the first 20 to 30 minutes of the test.

- Payload Mass Extinction Coefficient (αp)

Table 3 presents a summary of the αp data for the four new NWC pyrotechnics (LM 13, 14, 15 and 16) and phosphorus at the visible, 3-5 μm and 8-12 μm wavelength bands measured in high and low humidity tests. Also presented for comparison are previous data (Hanley et.al., 1983) obtained for the CY85A, LM9 and LM12 pyrotechnics. Table 4 presents the decay rate data, in terms of half-life, for αp and cloud mass for the four new pyrotechnics. Figure 3 presents the continuous αp spectra (visible to 14 μm) for the NWC and phosphorus smokes.

Several significant points are apparent from examination of Tables 3 and 4, and Figure 3:

- The carbonous smokes (LM 13 and 14) provide substantially greater IR wavelength extinction than the KCl smokes (LM 15 and 16). The carbonous smokes provide approximately five times greater IR extinction than the KCl smokes at high humidity, and up to approximately fifty times greater at low humidity.
- Under high humidity conditions at visible wavelengths, CY85A, LM9, LM14, LM15 and LM16 performed roughly comparibly with αp's ranging from 9.1 m^2/g for LM9 down to 7.1 m^2/g for LM16. The LM12 and 13 pyrotechnics were significantly less effective with αp's of 1.8 and ~4 m^2/g respectively. At low humidity, the LM9 smoke provided

Table 3
PAYLOAD MASS EXTINCTION COEFFICIENT (m^2/g)
OF THE NWC SMOKES

	HIGH HUMIDITY TESTS (80-90% RH)		
	VIS	3-5 μm	8-12 μm
LM13	~4	1.1	0.45
LM14	7.7	1.3	0.38
LM15	7.2	0.14	0.06
LM16	7.1	0.27	0.07
WP WEDGE	19.2	1.1	1.1
CY85A	7.3	0.17	0.07
LM9	9.1	0.25	0.09
LM12	1.8	0.99	0.26

	LOW HUMIDITY TESTS (~ 40% RH)		
	VIS	3-5 μm	8-12 μm
LM13	2.0	0.41	0.15
LM14	2.8	0.59	0.13
LM15	1.1	~ 0.02	~ 0.02
LM16	1.7	~ 0.02	< 0.01
WP WEDGE	11.1	0.89	0.67
CY85A	1.6	0.01	< 0.01
LM9	4.6	0.08	0.03
LM12	1.1	0.51	0.15

Table 4

HALF-LIFE (IN MINUTES) OF THE NWC SMOKES

		VIS	3-5 μm	8-12 μm	CLOUD MASS
HIGH HUMIDITY	LM13	X	36	17	32
	LM14	137	568	98	110
	LM15	224	–	–	–
	LM16	173	–	–	584
	WP WEDGE	X	–	–	X
LOW HUMIDITY	LM13	92	98	47	59
	LM14	91	–	–	315
	LM15	479	–	X	–
	LM16	252	–	X	294
	WP WEDGE	–	–	–	X

– DENOTES NO DECAY MEASURED

X DENOTES NO DATA AVAILABLE

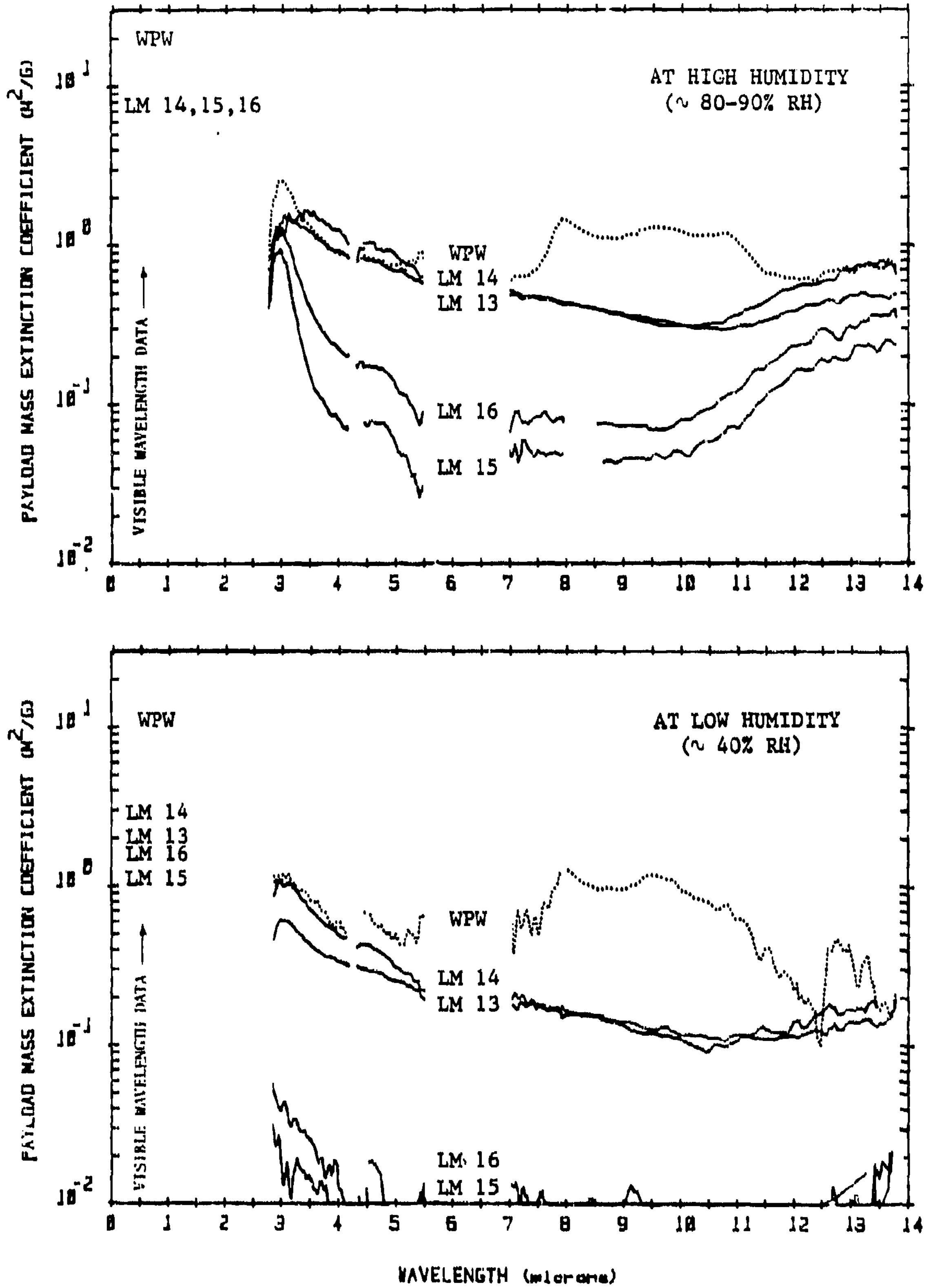

Figure 3. Extinction spectra (visible to 14 μm wavelength) of the NWC smokes at high and low humidity.

significantly greater extinction than any of the other NWC smokes tested having an αp value of 4.6 m^2/g as compared to 1.1-2.8 m^2/g for the other smokes.

- Of the carbonous smokes (LM 12, 13 and 14), LM14 is the most effective. All three have similar 3-5 µm and 8-12 µm αp's however LM14 has a significantly greater visible wavelength αp of ~7 m^2/g at high humidity and ~3 m^2/g at low humidity. These visible wavelength αp's are comparable to that for the NaCl/KCl smokes (CY85A, LM 15 and 16). Thus, the LM14 pyrotechnic provides substantially improved IR wavelength obscuration relative to the NaCl/KCl smokes while retaining the good visible wavelength extinction of the NaCl/KCl smokes.

- The use of the energetic binder in LM14 appears to be the cause of its improved extinction properties and slower decay rate relative to the non-energetic LM13. However, from these limited tests, the use of the energetic binder in LM16 does not appear to have significantly improved the extinction characteristics of the resultant smoke as compared to the non-energetic LM15.

- The decay rate of the LM13 pyrotechnic was the greatest of the smokes tested having a cloud mass half-life of approximately 30 mintues at high humidity.

3.4 Mass Yield and Aerosol Hygroscopicity

During tests 1 through 8, filter samples were drawn for assessment of mass yield and aerosol mass growth factors. Results from these measurements are presented in Table 5.

Perhaps the most significant finding is the increased mass yields of the energetic binder formulations, LM 14 and 16, relative to their non-energetic counterparts LM 13 and 15, respectively. Especially notable is the ~70% nominal mass yield of the LM14 pyrotechnic, approximately twice the yield of all previous NWC pyrotechnics.

Table 5

YIELD AND AEROSOL MASS GROWTH FACTORS OF THE NWC PYROTECHNICS

		PYROTECHNIC TOTAL MASS YIELD @ RH	PYROTECHNIC NOMINAL MASS YIELD	AEROSOL MASS GROWTH FACTOR
HIGH HUMIDITY	LM13	170%	39%	4.3
	LM14	257%	78%	3.3
	LM15	117%	28%	4.2
	LM16	162%	40%	4.1
	WP WEDGE	359%	59%	6.1*
	CY85A	143%	36%	4.0
	LM9	179%	22%	8.0
	LM12	130%	36%	3.6
LOW HUMIDITY	LM13	67%	48%	1.4
	LM14	105%	66%	1.6
	LM15	24%	22%	1.1
	LM16	44%	40%	1.1
	WP WEDGE	254%	65%	3.9*
	CY85A	38%	37%	1.1
	LM9	75%	27%	2.8
	LM12	68%	38%	1.8

*FROM TARNOVE, 1980.

The aerosol mass growth factors of the LM 13, 14, 15 and 16 smokes were approximately equivalent ranging from 3.3 to 4.3 at high humidity and from 1.1 to 1.6 at low humidity. Of all the NWC smokes, the LiCl smoke of the LM9 pyrotechnic underwent the greatest deliquescent growth having an aerosol mass growth factor of 8.0 at high humidity and 2.8 at low humidity.

3.5 Aerodynamic Size Distribution of the NWC Smokes

During the low humidity tests (tests 5 through 8) the size distribution of the smokes was evaluated with a six stage cascade impactor covering the size range from 0.5 to >16 µm equivalent aerodynamic diameter. The size distributions and associated equivalent aerodynamic mass median diameters (MMD) are presented in Figure 4. These distributions show the general difference between the carbonous (LM 13 and 14) and KCl (LM 15 and 16) smokes as well as possible influences of the energetic binders (LM 14 and 16) on particle size. These points are discussed further below.

From Figure 4, it is readily seen that the carbonous smokes (LM 13 and 14) have a significantly greater aerodynamic particle size than the KCl smokes (LM 15 and 16), consistent with both increased IR extinction and more rapid decay of the carbonous smokes relative to the KCl smokes.

Extracting information on the influence of the energetic binder on particle size is more difficult. The difficulty arises primarily due to the aerosol size distributions extending outside the sizing range of the impactor. For the carbonous smokes, the larger particles were not well sized due to the undefined upper limit of the first impaction stage collecting all particles >16 µm. For the KCl smokes, it appears that a large fraction of the aerosol was too small in diameter to be collected on the lowest stage (0.5-1 µm). It must also be realized when interpreting these data that in each case the sampling interval began 10 minutes after time zero (and lasted for 10 mintues). Thus, a fair fraction of the larger aerosol particles may have fallen out prior to sampling, particularly for the carbonous smokes.

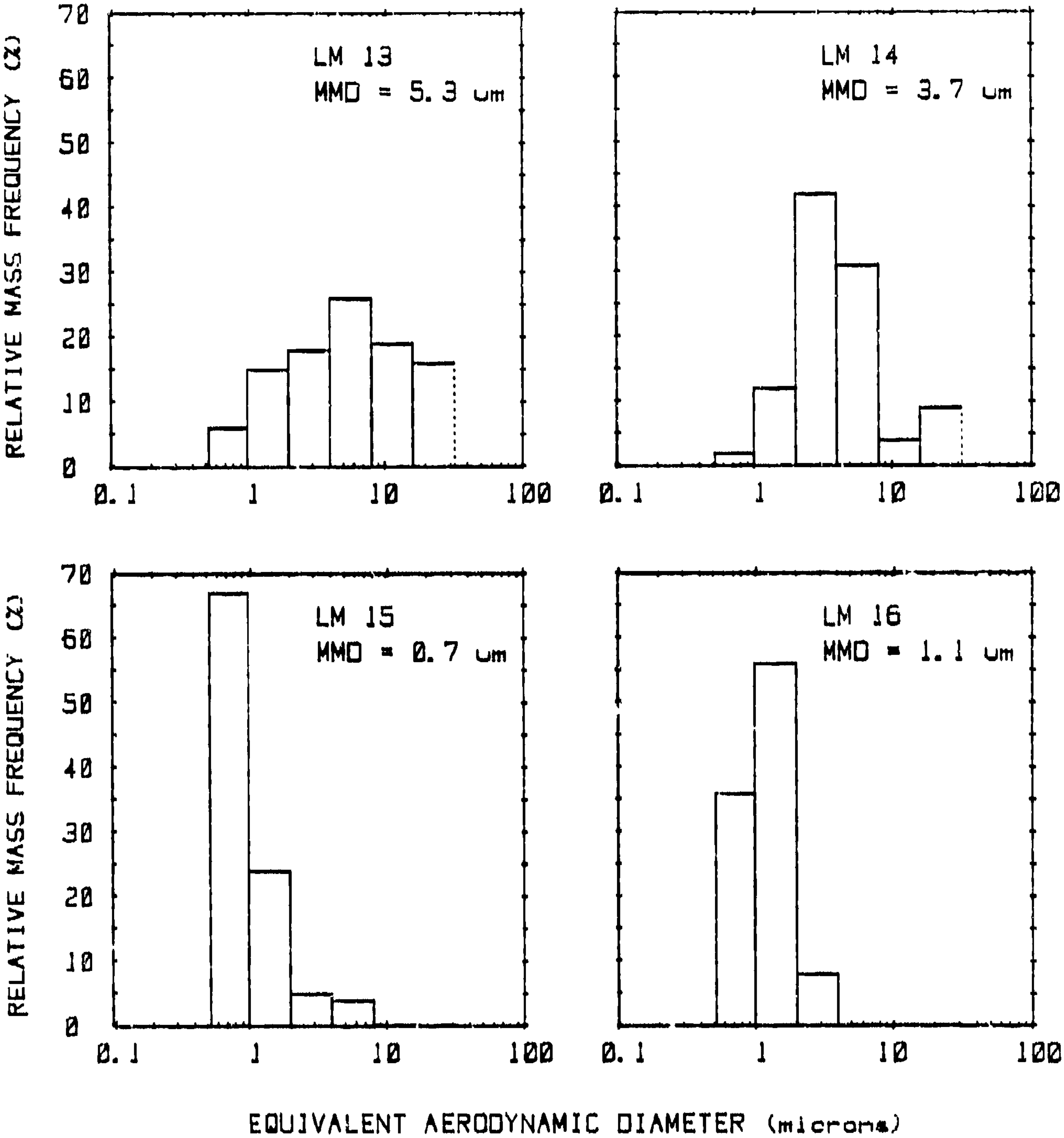

Figure 4. Relative size distributions of the NWC smokes (low humidity) derived from cascade impactor measurements.

With the above concerns in mind, the impactor data suggest that the use of the energetic binder in the carbonous formulations resulted in a decreased particle size, consistent with the reduced decay rate of the energetic formulation. For the KCl smokes, too much of the aerosol may have escaped collection to draw conclusions on the influence of the energetic binder from these measurements.

3.6 Particle Chemical Composition and Morphology

Subsequent to determining the aerosol mass collected upon each impactor stage, each stage was examined under the scanning electron microscope for determination of morphology and the elemental composition of the collected aerosol via energy dispersive x-ray analysis (for elements having atomic weights greater than sodium and less than uranium). The primary objective of this stage-by-stage analysis was to determine if particle composition varied with particle size and, specifically, to determine if in the carbonous smokes, the carbon and $MgCl_2$ exist as separate entities (with carbon comprising the larger particles and $MgCl_2$ the smaller) or if all the particles contain a mixture of $MgCl_2$ and carbon.

The results of the SEM analysis are presented in Table 6 where the major and minor components comprising the aerosol collected on each stage are given, as well as the mass fraction of the aerosol collected upon each stage (as was shown in Figure 4). Note that carbon, having an atomic weight less than that of sodium, was not analyzed in this procedure. However, visually the sample collected upon all stages of the LM13 and 14 carbonous smokes was black, indicating that carbon was present on each stage.

As can be seen in Table 6, no variation of particle composition with size was detected for the carbonous LM 13 and 14 smokes with each stage containing Mg, Cl and carbon (with traces of Si believed to be contaminate dust). Likewise, for the KCl smokes, LM 15 and 16, no significant variations were found, with the stages comprising the majority of the aerosol being composed of K and Cl. The other stages do show varying levels of Mg, Cl, K and Si but the mass fraction of the aerosol collected upon these larger-size stages is near zero making the measurements both difficult and of little or no practical significance.

Table 6
ANALYSIS OF CASCADE IMPACTOR DATA FOR THE NWC SMOKES

	STAGE	% MASS	MAJOR COMPONENT	MINOR COMPONENT
LM13	> 16	16%	Mg, Cl, C	TRACES OF Si
	8-16	19%		
	4-8	26%		
	2-4	18%		
	1-2	15%		
	0.5-1	6%		
LM14	> 16	9%	Mg, Cl, C	TRACES OF Si
	8-16	4%		
	4-8	31%		
	2-4	42%		
	1-2	12%		
	0.5-1	2%		
LM15	> 16	0%	TRACES OF K, Cl, Si	
	8-16	0%	Mg	K, Cl
	4-8	4%	Si	Mg, Cl, K
	2-4	5%	K, Cl	Mg
	1-2	24%	K, Cl	Mg
	0.5-1	67%	K, Cl	Mg
LM16	> 16	0%	K, Cl, Si	Mg
	8-16	0%	Mg	Cl, K, Si
	4-8	0%	Mg, Cl, K	Si
	2-4	8%	Mg, Cl, K	–
	1-2	56%	K, Cl	Mg
	0.5-1	36%	K, Cl	Mg

To further examine the particle morphology of the smokes, particularly of the carbonous smokes, filter samples were drawn during tests 5 through 8 for examination under the electron microscope. Representative photomicrographs are presented in Figure 5 for each of these tests. For the carbonous smoke samples of LM 13 and 14, most of the particles were found to be aggregates composed of two componenets: solid, roughly spherically shaped particles identified as $MgCl_2$ (via energey dispersive x-ray analysis) and sooty chained particles identified as being carbonous (based on particle morphology, color and NWC's predictive thermochemistry computer program). Close examination of the LM 13 and 14 samples showed that the $MgCl_2$ particles were nearly always found in contact with the carbonous particles. This, together with the impactor data, strongly suggests that carbon and $MgCl_2$ coexist in each smoke particle. Mixed-composition particulates may be the result of coagulation of the $MgCl_2$ and carbonous particles or perhaps results from the $MgCl_2$ vapors condensing directly upon the carbonous particles as the smoke is being generated.

3.7 Burn Rate of the NWC Pyrotechnics

The use of the energetic binder significantly increased the burn rate of the LM 14 and 16 pyrotechnics over that of their non-energetic counterparts. Burn rates for the NWC pyrotechnics derived from tests 1 through 8, and for the phosphorus payloads for tests 12 and 13, are presented in Table 7. Also presented is the burn rate for the 160 lb CY85A canisters combusted during NRL's at-sea trial of the CY85A pyrotechnic (Hanley, et.al. 1984). The burn rates presented in Table 7 must be interpreted with the understanding that burn rate is likely to be both surface area and payload mass dependent. Thus, the rates reported are strictly applicable only to the payloads used in these tests.

As can be seen from Table 7, of the four new NWC pyrotechnics, the energetic LM 14 and 16 pyrotechnics had the highest burn rates — 320 and 480 g/min., respectively. The increase in burn rate with payload size is clearly demonstrated by the 9072 g/min burn rate of the 160 lb CY85A payloads compared to that for an 80 g payload of $\sim$120 g/min.

Also denoted in Table 7 is the burn rate for a 23.5 g payload of munition grade white phosphorus felt wedge having a burn rate of $\sim$3 g/min. The relatively slow burn rate of the phosphorus suggests that one aspect of the NWC smokes which might be exploited is their more rapid burn rate (approximately two orders of magnitude greater than phosphorus). For example, in field applications,

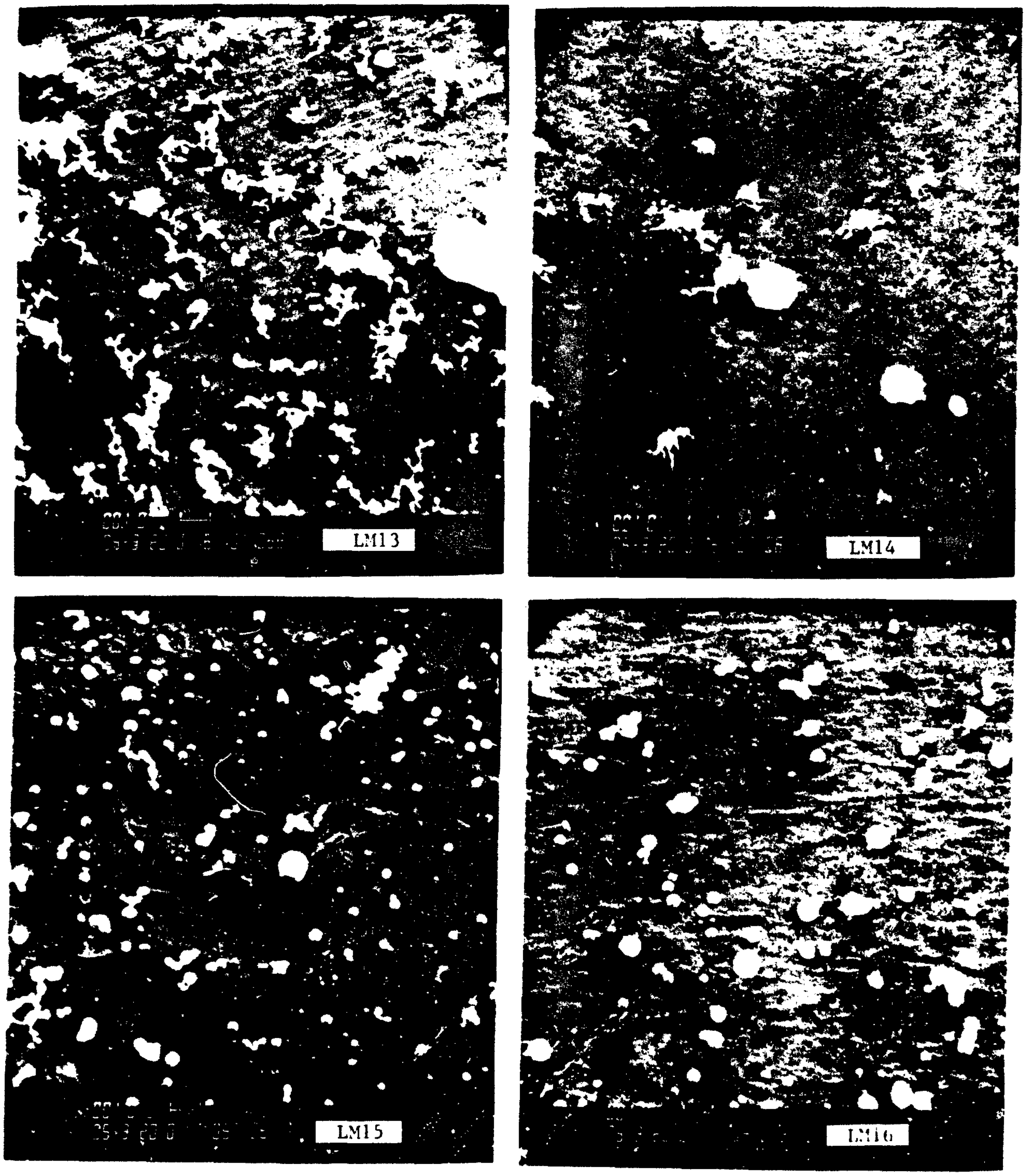

Figure 5. Photomicrographs of aerosol filter samples drawn from the NWC smokes. Note the 1 micron sizing bar in each photo.

Table 7
BURN RATES OF THE NWC PYROTECHNICS

PAYLOAD		BURN RATE (g/min)
80g	LM9	51
80g	LM12	–
80g	LM13	40
80g	LM14	320
80g	LM15	120
80g	LM16	480
23.5g	WP WEDGE	2.9
80g	CY85A	~ 120
72,600g	CY85A*	9072

*FROM AT-SEA TESTS WITH 160 POUND PAYLOADS OF CY85A (HANLEY ET AL., 1983)

the NWC smokes may be able to produce smoke plumes of greater obscuration than those generated by phosphorus munitions due to the capability of the NWC pyrotechnics to disseminate the obscurant material faster, thereby forming a more concentrated smoke plume.

3.8 Mass Balance

As a check on our experimental procedures and control, a mass balance assessment was performed. For tests 1 through 8, the payload mass, a controlled quantity accurately measured prior to each test, was compared to the summation of the various masses measured or estimated after pyrotechnic combustion. These post combustion masses include: 1) the nominal aerosol mass of the smoke produced as determined from the mass loading filter samples, 2) the mass of the unaerosolized material determined by weighing the residual matter remaining in the combustion bowl after pyrotechnic combustion, and 3) the mass of gas produced by the pyrotechnic as provided by NWC's thermochemistry computer program.

The results of the mass balance evaluation, presented in Table 8, show that on average approximately 97% of the payload mass was accounted for in the post combustion evaluation.

Table 8

MASS BALANCE

TEST NO.	PAYLOAD	PERCENT OF PAYLOAD MASS						
		RESIDUE	+	NOMINAL AEROSOL	+	GAS	=	TOTAL
1	80g LM13	33	+	39	+	9	=	81
2	80g LM14	14	+	78	+	22	=	114
3	80g LM15	19	+	28	+	52	=	99
4	80g LM16	7	+	40	+	50	=	97
5	80g LM13	39	+	48	+	9	=	96
6	80g LM14	6	+	66	+	22	=	94
7	80g LM15	19	+	23	+	52	=	94
8	80g LM16	7	+	40	+	50	=	97

SECTION 4

ENHANCEMENT OF THE IR WAVELENGTH EXTINCTION OF DELIQUESCED SMOKE AEROSOL THROUGH THE USE OF POLYMER SURFACE ACTIVE AGENTS.

4.1 Objective

The objective of this task was to initiate an investigation into the potential use of IR absorbing polymers to coat the surface of hygroscopic aerosol so as to increase the IR extinction of the aerosol as well as to inhibit droplet evaporation. Previous studies by Calspan (Mack et.al., 1978) and NRL (Gathman et.al., 1979) demonstrated a limited utility of cetyl alcohol to coat deliquesced aerosol resulting in decreased evaporation upon exposure to decreasing relative humidity. The present task extends the cetyl alcohol studies by using IR absorbing material as the coating agent. In this way, not only might aerosol droplet evaporation be reduced but, more significantly, the IR extinction of the smoke aerosol may be increased.

4.2 Procedure

Evaluation procedures for the present task were directed towards finding polymers which demonstrated the ability to form a non-volatile coating on deliquesced aerosol droplets. While the polymers evaluated have properties which should lead to increased IR absorption, IR absorption measurements were not part of this initial evaluation.

To assess the formation of a non-volatile skin on deliquesced aerosol, the extinction (visible wavelength) of a deliquesced aerosol smoke cloud was monitored as a function of decreasing relative humidity. During such a test, uncoated aerosol droplets will undergo significant evaporation resulting in decreased extinction whereas an aerosol effectively coated will undergo little or no evaporation with extinction remaining nearly constant as the humidity is lowered.

The tests were conducted in a small (0.06 m^3) chamber with 20 mg charges of the CY85A pyrotechnic used to generate the deliquescent aerosol smoke. Initially, the chamber was at high humidity (RH>95%). After combustion of the

pyrotechnic and allowing two minutes for the smoke to become uniformly distributed in the chamber, vapors of the candidate polymer were injected into the chamber. Following vapor injection, dry air was slowly pumped into the chamber to effect a gradual reduction of relative humidity over a 30 minute test period. The decrease of extinction as a function of time (and hence RH) for coated and non-coated (control tests) aerosol were compared to determine the effectiveness of various polymers. A total of fifteen polymers were screened with this procedure.

4.3 Results

During the analysis of the test data, it became apparent that the measured decreases in extinction were not directly related to decreases in relative humidity. Several sources of error inherent to the design of the test chamber are believed to have contributed to this including the dilution of the smoke upon introduction of the dry air, the presence of excess water for evaporation into the dry air thereby maintaining high humidity conditions, and the gravitational settling of the aerosol droplets contributing to the decrease of extinction. As a result of these sources of error, definite conclusions on the coating ability of the polymers cannot be drawn from this initial investigation. However, even with these uncertainties, the results suggest that four of the evaluated polymers may have successfully coated the aerosol: dimethyldichlorosilane, chloropropyltrichlorosilane, 3-heptafluoro (isopropoxy) dimethylsilane (called "3-HEPT.", and poly-bis)p-toluene sulfonate diacetylene.

Design improvements for the test apparatus which would eliminate or minimize known sources of error have been considered. It is recommended that these design changes be implemented and that the polymers be re-evaluated to quantify their surface coating ability. Following successful tests, the polymers should be further evaluated in larger scale chamber tests to assess their potential to increase the IR extinction of the smoke aerosol.

SECTION 5

CONCLUSIONS AND RECOMMENDATIONS

5.1 Conclusions

The principal conclusions drawn from this year's effort are:

1. At IR wavelengths, the carbonous smokes (LM 13 and 14) provide substantially greater extinction than the KCl smokes (LM 15 and 16). The carbonous smokes provide approximately five times greater IR extinction than the KCl smokes at high humidity, and up to approximately fifty times greater IR extinction at low humidity.

2. Of the carbonous smokes, LM14 is the most effective; all have similar 3-5 μm and 8-12 μm αp's, however LM14 has a significantly greater visible wavelength αp of $\sim 8\ m^2/g$ at high humidity and $\sim 3\ m^2/g$ at low humidity. These visible wavelength αp's are comparable to that for the NaCl/KCl smokes (CY85A, LM 15 and 16). Thus, the LM14 pyrotechnic provides substantially improved IR wavelength obscuration relative to the NaCl/KCl smokes while reproducing the good visible wavelength extinction of these smokes.

3. The pyrotechnic nominal mass yield of LM 14 averaged 72%, approximately twice that of all previous NWC pyrotechnics.

4. At visible wavelengths, under high humidity conditions, CY85A, LM9, LM14, LM15 and LM16 performed roughly comparably with αp's ranging from $9.1\ m^2/g$ for LM9 down to $7.1\ m^2/g$ for LM16. The LM 12 and 13 pyrotechnics were significantly less effective with αp's of 1.8 and $\sim 4\ m^2/g$, respectively.

At visible wavelengths under low humidity conditions, the LM9 smoke provided significantly greater extinction than any of the other NWC smokes tested, having an αp value of $4.6\ m^2/g$ as compared to $1.1\text{-}2.8\ m^2/g$ for the other smokes.

5. For the carbonous smoke producing pyrotechnics, the use of the energetic binder in LM14 appears to be the cause of its improved extinction properties and slower aerosol decay rate relative to the non-energetic LM13. For the KCl smokes, however, the use of the energetic binder in LM16 does not appear to have significantly improved th extinction characteristics of the resultant smoke as compared to the non-energetic LM15.

6. The decay rate of the LM13 pyrotechnic was the greatest of the smokes tested having a cloud mass half-life of approximately 30 minutes at high humidity, probably the result of larger particles produced by this pyrotechnic.

7. The magnesium chloride and carbon components of the carbonous smokes appear to coexist in each aerosol particle.

8.. The bulk density of the carbonous smoke producing LM 13 and 14 pyrotechnics was approximately half of that of the other NWC pyrotechnic.

5.2 Recommendations

The recently developed LM14 pyrotechnic represents a significant and substantial improvement to the extinction properties of the NWC smokes relative to the original CY85A pyrotechnic. Further improvements in smoke performance may yet be possible through two approaches. First, through control of the particle size generated by the pyrotechnic, particle size could be optimized for scattering at specific wavelength regions such as the 8-12 μm band. For water droplets (spherical shape with a refractive index of 1.3) the optimum particle size for scattering radiation of a given wavelength occurs when the particle radius and wavelength are roughly equal. For the pyrotechnic smokes, particularly the carbonous smokes having irregular particle shape and uncertain refractive index, the relationship between particle size and scattering will need to be determined through a combined experimental and theoretical evaluation. The second approach to increase the smoke's performance is to incorporate IR absorbing substances into the smokes. This approach could be directed towards a general increase in extinction at IR wavelengths (2-14 μm) or be targeted to specific wavelengths, e.g., 10.6 μm - the operating wavelength of CO_2 lasers. To aid in directing the above efforts to improve smoke performance, a theoretical and experimental study should be performed to determine the relative contributions of scattering and absorption to the extinction of the present NWC smokes and to assess the maximum contribution which scattering and absorption can each provide.

In general, the recently developed NWC pyrotechnics are comparable to phosphorus and other military obscurants (e.g. fog oil and EA5763) in obscuration potential at visible and IR wavelengths. It is interesting to note that fog

oil, only a relatively fair obscurant at visible wavelength and poor at IR wavelengths, is perhaps the most widely used military obscurant (U.S. as well as Soviet); use of existing inventory phosphorus smokes or of the present NWC smokes would provide greater obscuration per unit payload. Apparently, logistics considerations and/or dissemination properties play an important role in the continued use of fog oil. Thus, along with further improvements in the extinction potential of the NWC smokes, consideration should also be given to the special and unique properties of the NWC pyrotechnics and their smokes which are not offered by other obscurants.

Several properties of the NWC pyrotechnics may be advantageous in certain situations. For example, the rapid burn rate of the pyrotechnics would be advantageous for use when smoke munitions must be exploded over water where, for maximum effectiveness, combustion of the smoke producing fragments must be completed before they are quenched in the sea. The rapid burn rate suggests usage as a propellent in "smoke rockets" designed to rapidly lay out extensive smoke screen curtains (Reference 12). The emissive nature of the carbonous NWC smokes may provide unique capabilities as thermal obscurants and decoys to defeat IR systems (References 7, 8 and 9). Also, the non-toxic nature of the CY85A and similar smokes suggests that they may be valuable in training exercises. These, and other, potential uses should be considered for the NWC smokes with further development and evaluation directed at the most promising applications.

Based on the results of this year's program, our previous work and the above discussion, the following recommendations are presented:

1. To aid in further improving the extinction performance of the NWC smokes, a theoretical and/or experimental study should be performed to determine the actual and potential contribution of scattering and absorption to extinction in the NWC smokes.

2. A theoretical and experimental study should be initiated to determine the processes which influence the particle size of the NWC pyrotechnic smokes and to examine how these processes can be controlled.

3. Continue investigation into the use of IR absorbing surface active agents to increase the IR extinction of the NWC smokes.

4. Investigate the thermal emission (8-12 μm wavelength) characteristics of the carbonous NWC smokes. These measurements should be designed to differentiate the contribution to the emission of heat associated with combustion, hydration and condensation.

5. Investigate potential deployment concepts of the NWC pyrotechnics which would take advantage of unique or superior performance properties not available with other obscurants.

6. As use of the carbonous NWC smokes continues, an evaluation should be made of possible adverse health effects associated with inhalation of these smokes.

REFERENCES

1. Mack, E.J., Anderson, R.J. and Hanley, J.T., 1978: "A Preliminary Investigation of the Production of Stable Fogs Under Subsaturated Conditions," Calspan Report No. 6287-M-1, 103 pp, Calspan Corporation, Buffalo, NY 14225

2. Mack, E.J. and Hanley, J.T., 1980: "A Laboratory Study of Artificial Fogs Produced Under Subsaturated Conditions," Calspan Report No. 651--M-1, 37 pp, Calspan Corporation, Buffalo, NY 14225.

3. Hanley, J.T. and Mack, E.J., 1980: "A Laboratory Investigation of Aerosol and Extinction Characteristics for Salty Dog, NWC 29 and NWC 78 Pyrotechnics," Calspan Report No. 6665-M-1, 40 pp, Calspan Corporation, Buffalo, NY 14225.

4. Hanley, J.T., Wattle, B.J. and Mack, E.J., 1981: "Extinction Characteristics of Pyrotechnically-Generated Alkali-Halide Smokes," Calspan Report No. 6855-M-1, 39 pp, Calspan Corporation, Buffalo, NY 14225.

5. Hanley, J.T., Kile, J.N., Wattle, B.J. and Mack, E.J., 1983: "IR and Visible Wavelength Obscuration by Pyrotechnically Generated Alkali Halide Smokes," Calspan Report No. 7031-M-1, 26 pp, Calspan Corporation, Buffalo, NY 14225.

6. Hanley, J.T., Mack, E.J. and Wattle, B.J., 1983: "At-Sea Evaluation of the Obscuration Characteristics of a Hygroscopic Aerosol Smoke Produced by the CY85A Pyrotechnic," Calspan Report No. 7031-M-2, 45 pp, Calspan Corporation, Buffalo, NY 14225.

7. Hanley, J.T., T.M. Albrechcinski, W.H. Wurster and G. Herman, "Facility for Ranking Emissive Smoke Perofrmance", Presented at the Smoke/Obscurants Symposium VIII, Adelphi, MD 17-19 April 1984.

8. Dinerman, C., Mathews, L., Cronin, H., and Ladouceur, H.D., "An Experiment to Identify the Mechanisms of Infrared Smoke EMission", Presented at the Smoke/Obscurants Symposium IX, Adelphi, MD, 1985.

9. Mathews, L., Reed, R., Dinerman, C. and St. Amand, P., "Heat Emitting Smoke Formulations", Presented at the Smoke/Obscurants Symposium IX, Adelphi, MD, 1985.

10. Tarnove, T.L., 1980: "Studies of the Chemistry of the Formation of Phosphorus-Derived Smokes and Their Implications for Phosphorus Smoke Munitions, " ARCSL-TR-80049.

11. Gathman, S.G., Julian, B.G., Markson, R.K. and Sedlacek, J., "Field Test of the Stabilization of Supersized Water Droplets Condensed on Pyrotechnically Generated Hygroscopic Nuclei," NRL Memorandum Report No. 4059, 26 pp., Naval Research Laboratory, Washington, D.C., 1979.

12. Mathews, L.A. and P. St. Amand, "Alkali Halide and Magnesium Chloride Smokes," Proceedings of the Smoke/Obscurants Symposium VI, April 1982.

APPENDIX A

EXTINCTION AND MASS YIELD PARAMETERS

There are numerous parameters which may be used to characterize the extinction effectiveness of an obscurant. Which parameter, or combination of parameters, is chosen will depend upon the specific applications involved. In the development of an obscurant, it is often desirable to separate the effects of dissemination efficiency and aerosol extinction. By doing so, each phase may be evaluated, studied and improved separately. Additionally, this allows for comparison to other obscurants which may differ fundamentally in the means of dissemination and/or aerosol properties.

When discussiong hygroscopic aerosols, confusion sometimes occurs with reference to "aerosol mass" as to whether this is to include mass resulting from processes such as oxidation, hydration and condensation or, is solely the mass of the aerosol which originated from the pyrotechnic. To avoid this confusion in this report, the term "total aerosol mass" will refer to the entire aerosol mass. The term "nominal aerosol mass" will refer only to the aerosol mass which originated directly from the pyrotechnic and will not include, therefore, any additional mass as may be supplied by the environment. Thus, for the alkali-halide aerosols, the nominal mass is the total aerosol mass minus the mass of condensed water; for a phosphorus smoke aerosol, the nominal mass would be the total aerosol mass minus the mass due to oxidation, hydration and condensation.

In light of the above, extinction measurements are reported in terms of both a dissemination efficiency and an aerosol extinction parameter. Dissemination efficiency is presented in terms of the pyrotechnic nominal mass yield computed from

NOMINAL MASS YIELD = (NOMINAL AEROSOL MASS)/(PAYLOAD MASS).

Extinction measurements are presented in terms of the payload mass extinction coefficient computed from

$$\text{PAYLOAD MASS EXTINCTION COEFFICIENT} = \frac{\text{(EXTINCTION COEFFICIENT)}}{\text{(PAYLOAD MASS PER UNIT CLOUD VOLUME)}}$$

When dealing ·ith a deliquescent aerosol, where particle size and, hence, extinction, is a function of humidity, a measure of the aerosol growth is useful in interpreting the extinction data. Aerosol growth will be represented by the aerosol mass growth factor computed from

AEROSOL MASS GROWTH FACTOR = (TOTAL AEROSOL MASS)/(NOMINAL AEROSOL MASS).

Also, the added mass due to condensation will increase the total mass yield of the pyrotechnic. This is reported as the pyrotechnic total mass yield computed from

PYROTECHNIC TOTAL MASS YIELD (@ RH) = (TOTAL AEROSOL MASS (@ RH)/(PAYLOAD MASS).

APPENDIX B

Plots of the payload mass extinction coefficient at
visible, 3-5 μm and 8-12 μm wavelengths
and aerosol mass loading as a function of time.

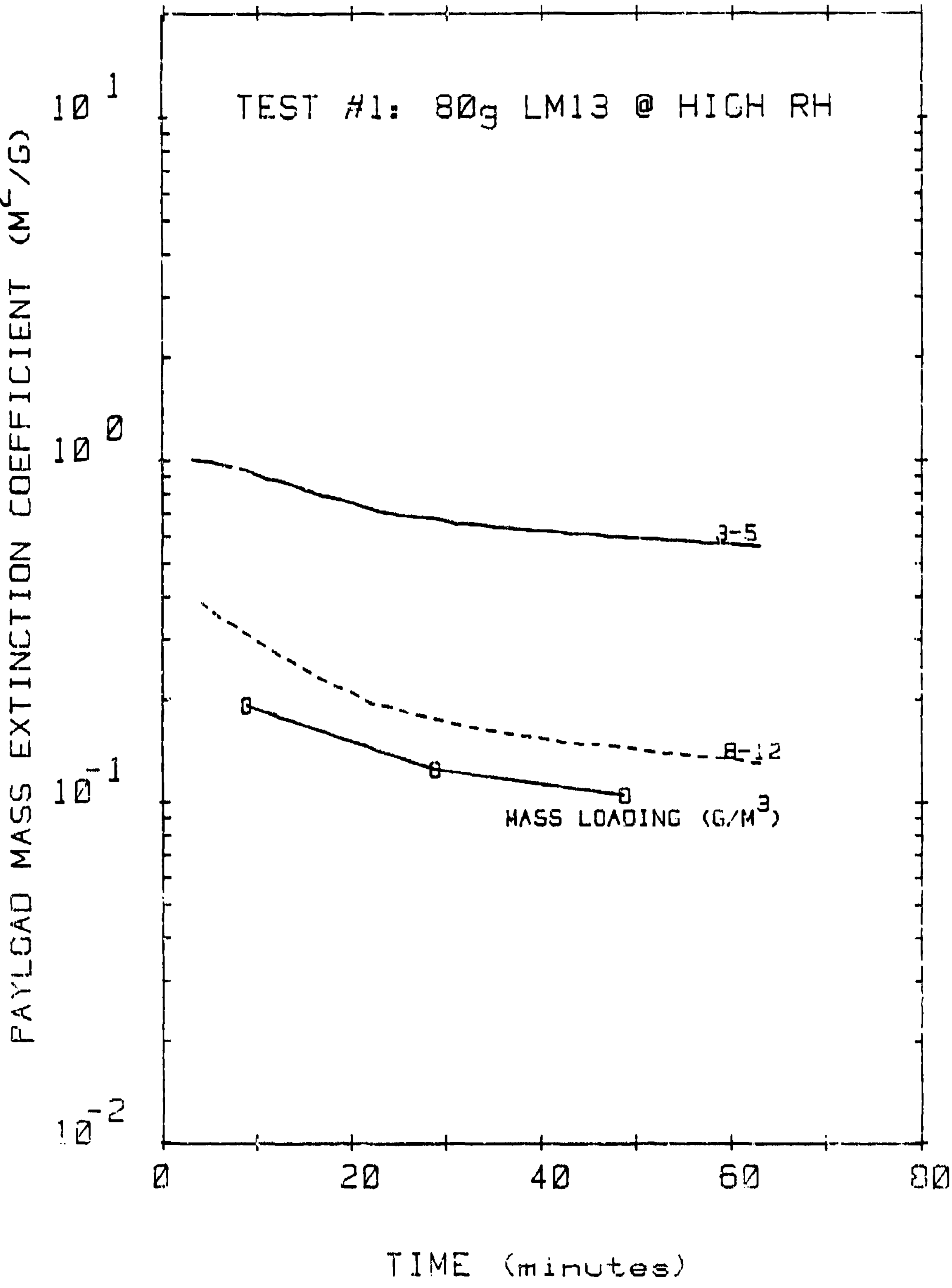
TEST #1: 80g LM13 @ HIGH RH
PAYLOAD MASS EXTINCTION COEFFICIENT (M^2/G)
10^1
10^0
10^{-1}
10^{-2}
3-5
8-12
MASS LOADING (G/M^3)
0
20
40
60
80
TIME (minutes)

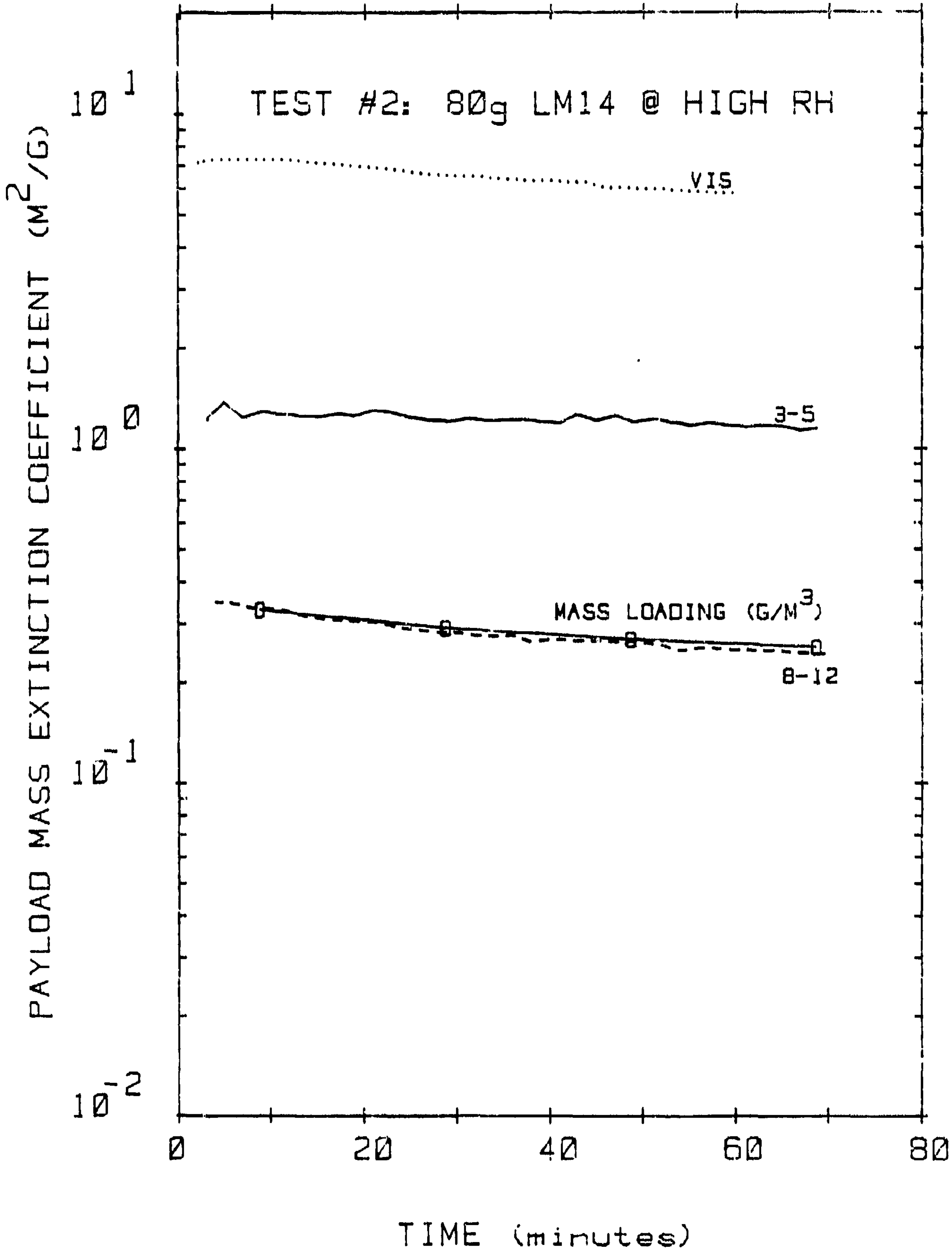
TEST #2: 80g LM14 @ HIGH RH
VIS
3-5
MASS LOADING (G/M3)
8-12
PAYLOAD MASS EXTINCTION COEFFICIENT (M2/G)
10 1
10 0
10 -1
10 -2
0
20
40
60
80
TIME (minutes)

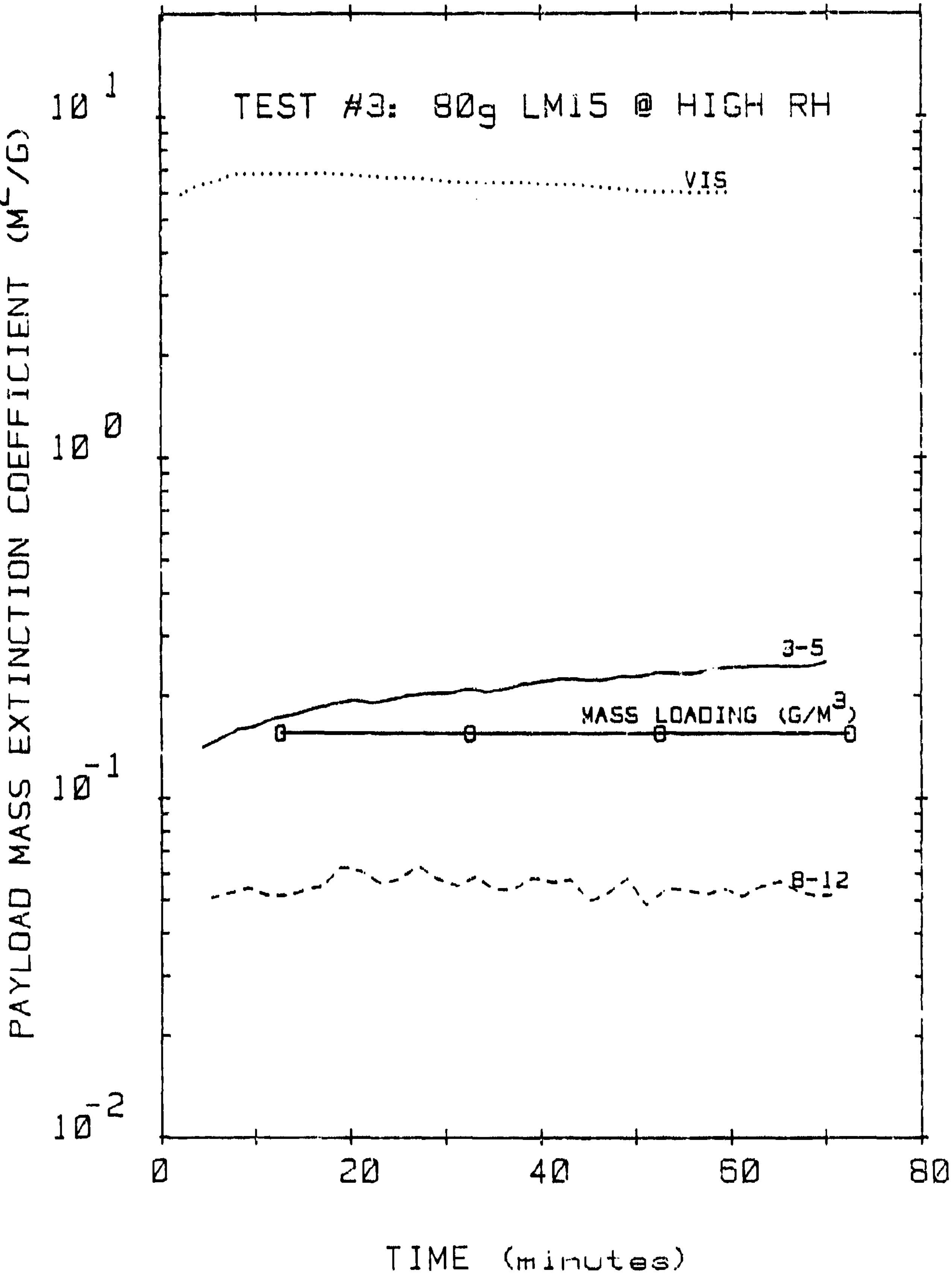
TEST #3: 80g LM15 @ HIGH RH
VIS
3-5
MASS LOADING (G/M3)
8-12
10 1
10 0
10 -1
10 -2
PAYLOAD MASS EXTINCTION COEFFICIENT (M2/G)
0
20
40
60
80
TIME (minutes)

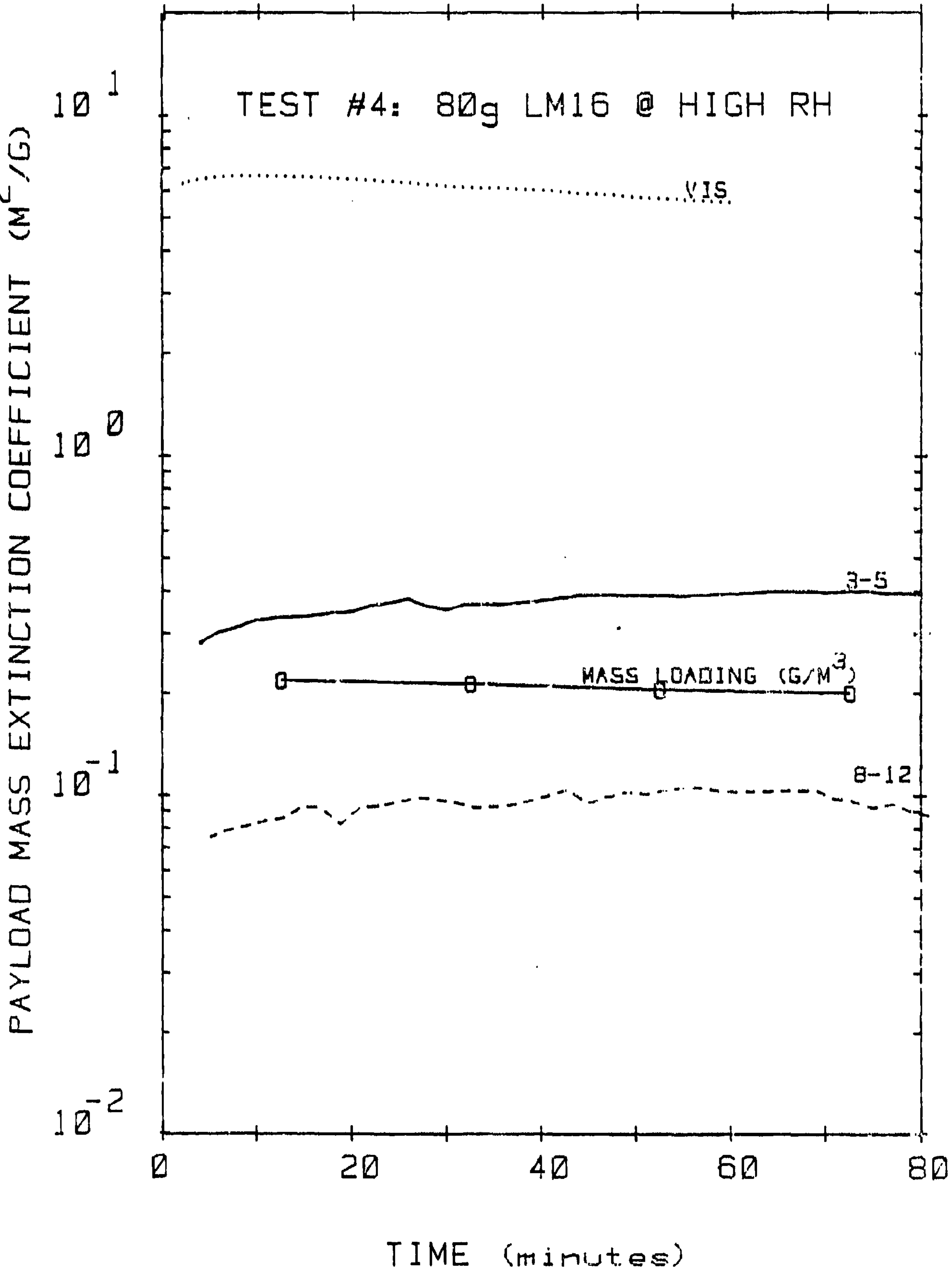
TEST #4: 80g LM16 @ HIGH RH
PAYLOAD MASS EXTINCTION COEFFICIENT (M^2/G)
10^1
10^0
10^-1
10^-2
VIS
3-5
MASS LOADING (G/M^3)
8-12
0
20
40
60
80
TIME (minutes)

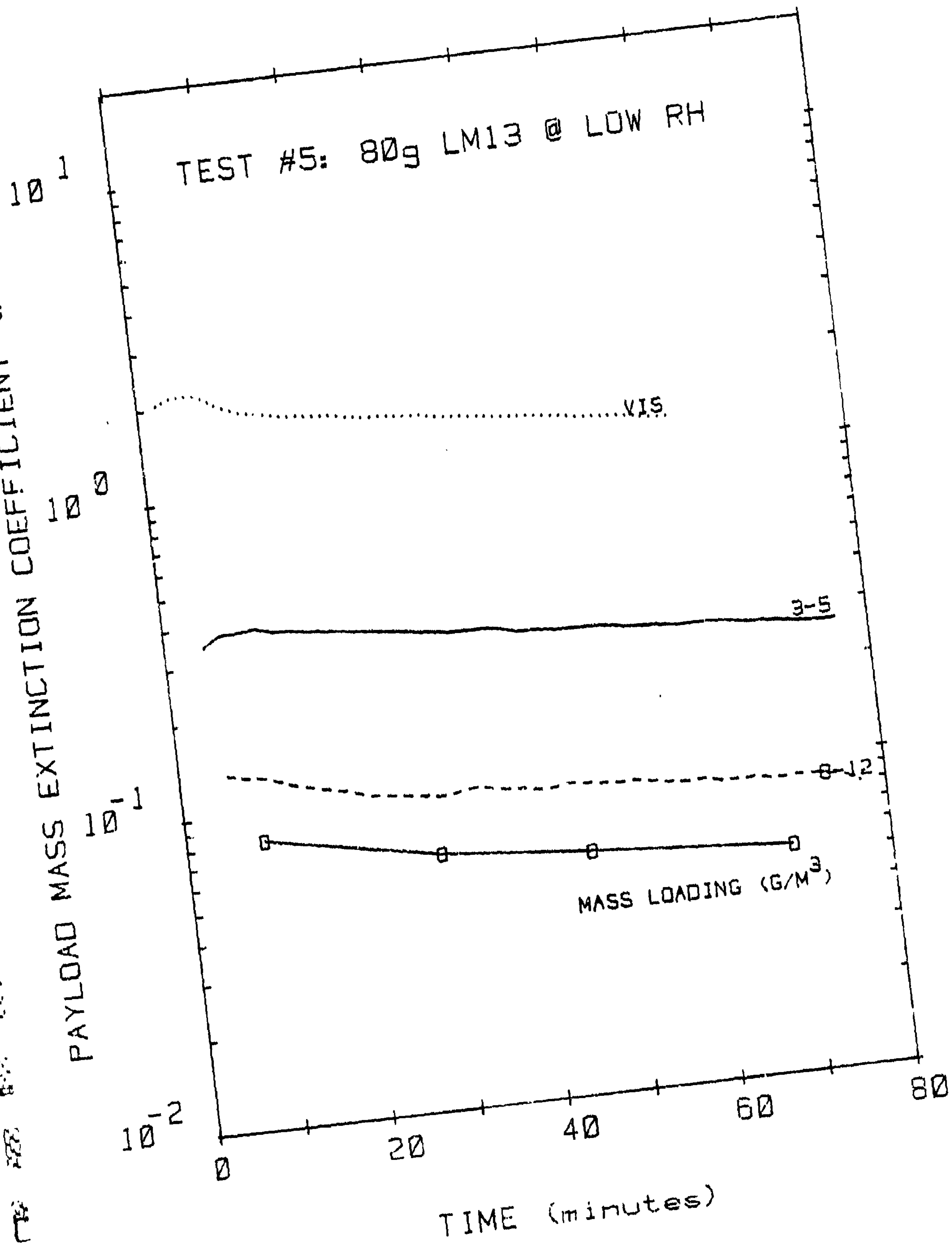
TEST #5: 80g LM13 @ LOW RH
PAYLOAD MASS EXTINCTION COEFFICIENT (M^2/G)
10^1
10^0
10^-1
10^-2
VIS
3-5
12
MASS LOADING (G/M^3)
0
20
40
60
80
TIME (minutes)

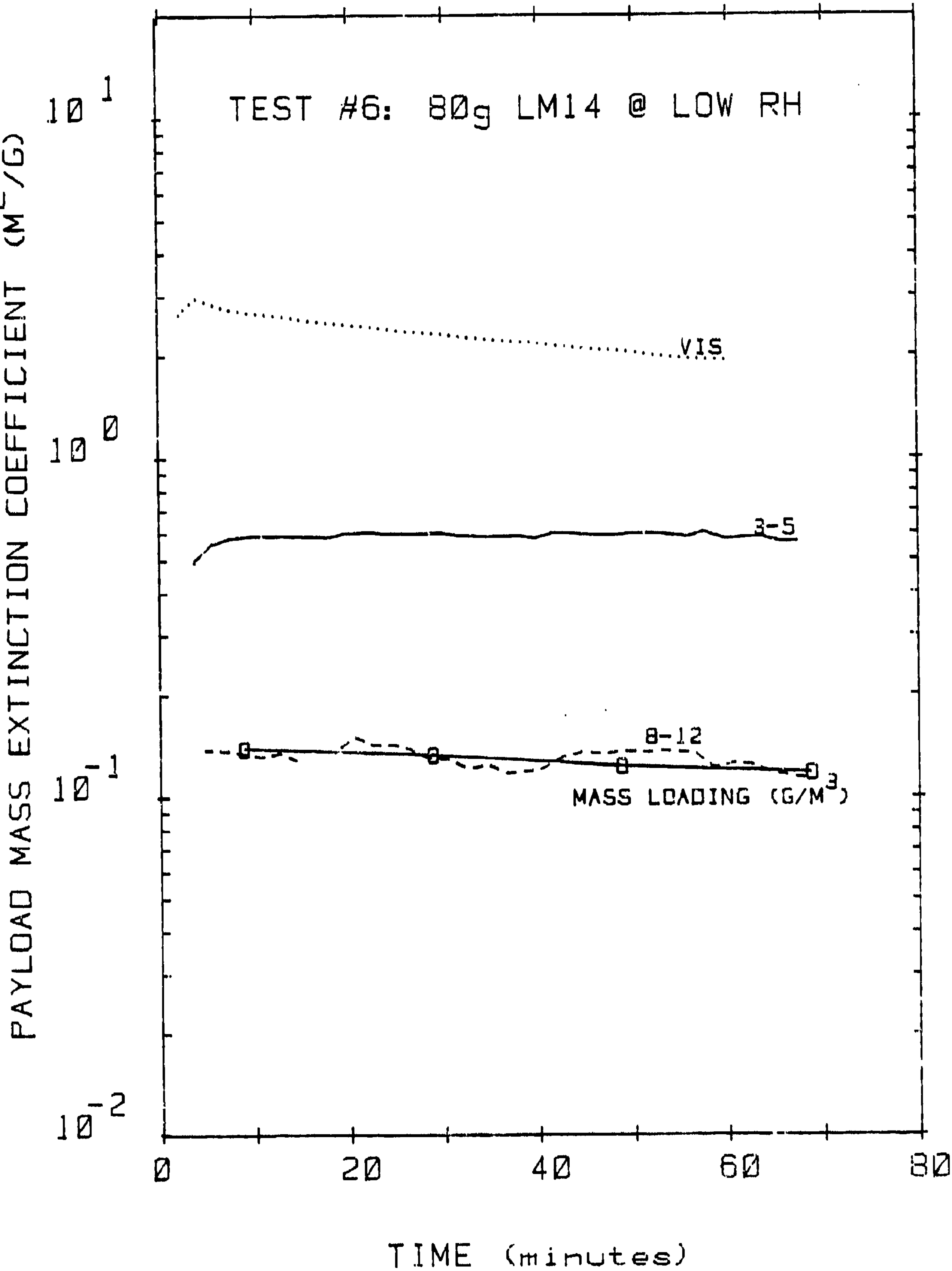

TEST #6: 80g LM14 @ LOW RH
PAYLOAD MASS EXTINCTION COEFFICIENT (M²/G)
10¹
10⁰
10⁻¹
10⁻²
VIS
3-5
8-12
MASS LOADING (G/M³)
0
20
40
60
80
TIME (minutes)

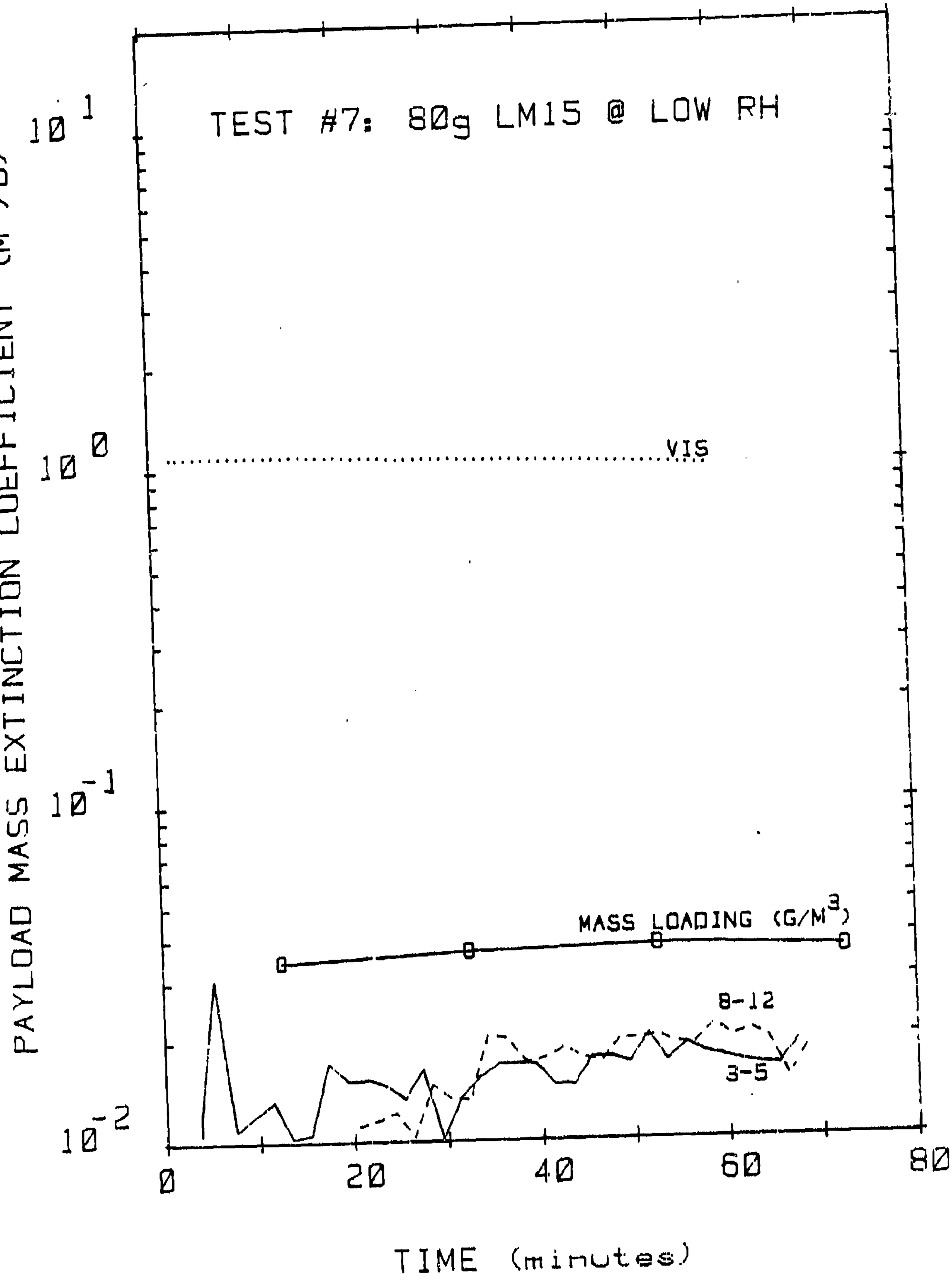
TEST #7: 80g LM15 @ LOW RH
PAYLOAD MASS EXTINCTION COEFFICIENT (M²/G)
10 1
10 0
10 -1
10 -2
VIS
MASS LOADING (G/M³)
8-12
3-5
0
20
40
60
80
TIME (minutes)

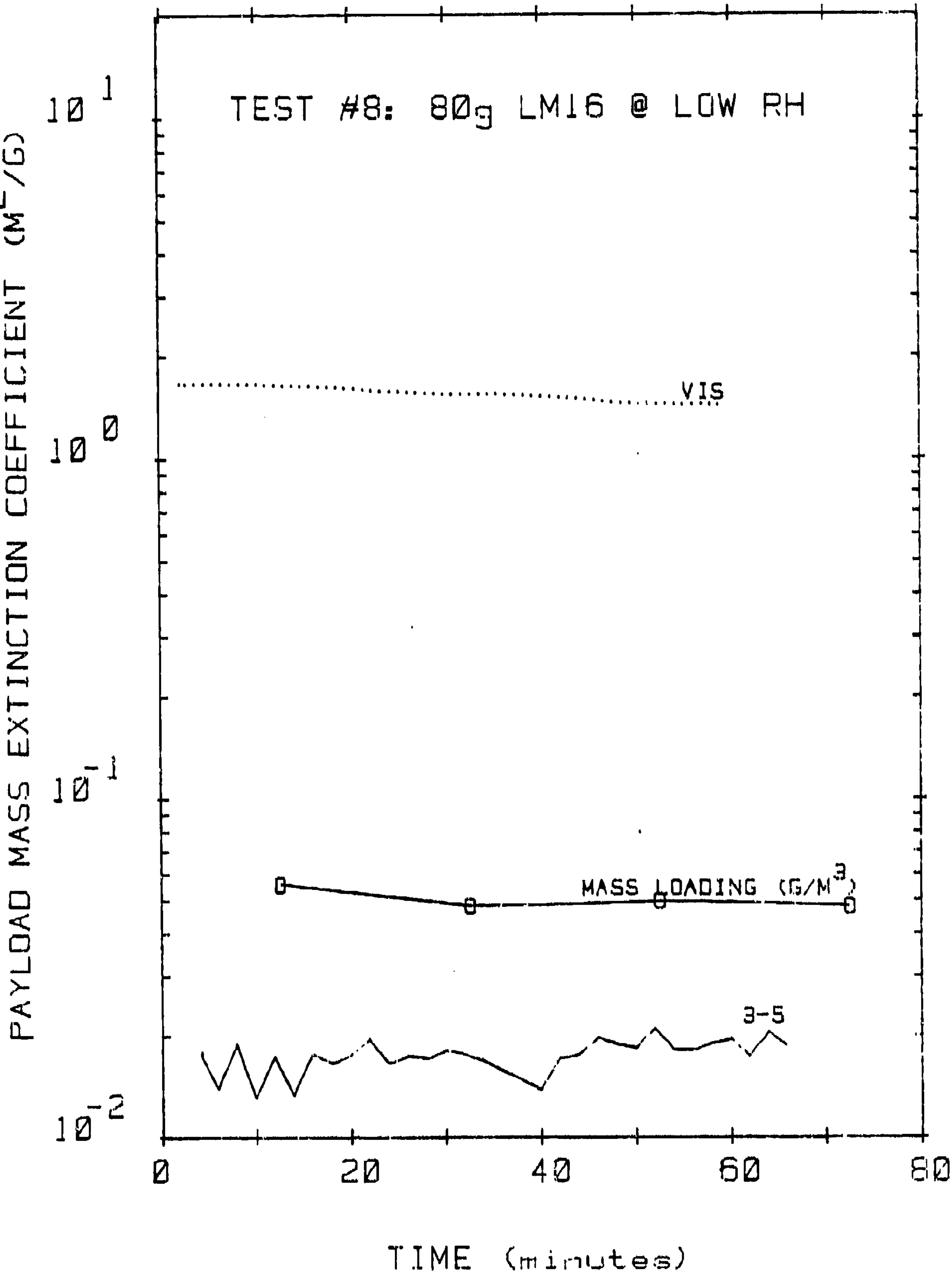
TEST #8: 80g LM16 @ LOW RH
PAYLOAD MASS EXTINCTION COEFFICIENT (M²/G)
10 1
10 0
10 -1
10 -2
VIS
MASS LOADING (G/M³)
3-5
0
20
40
60
80
TIME (minutes)

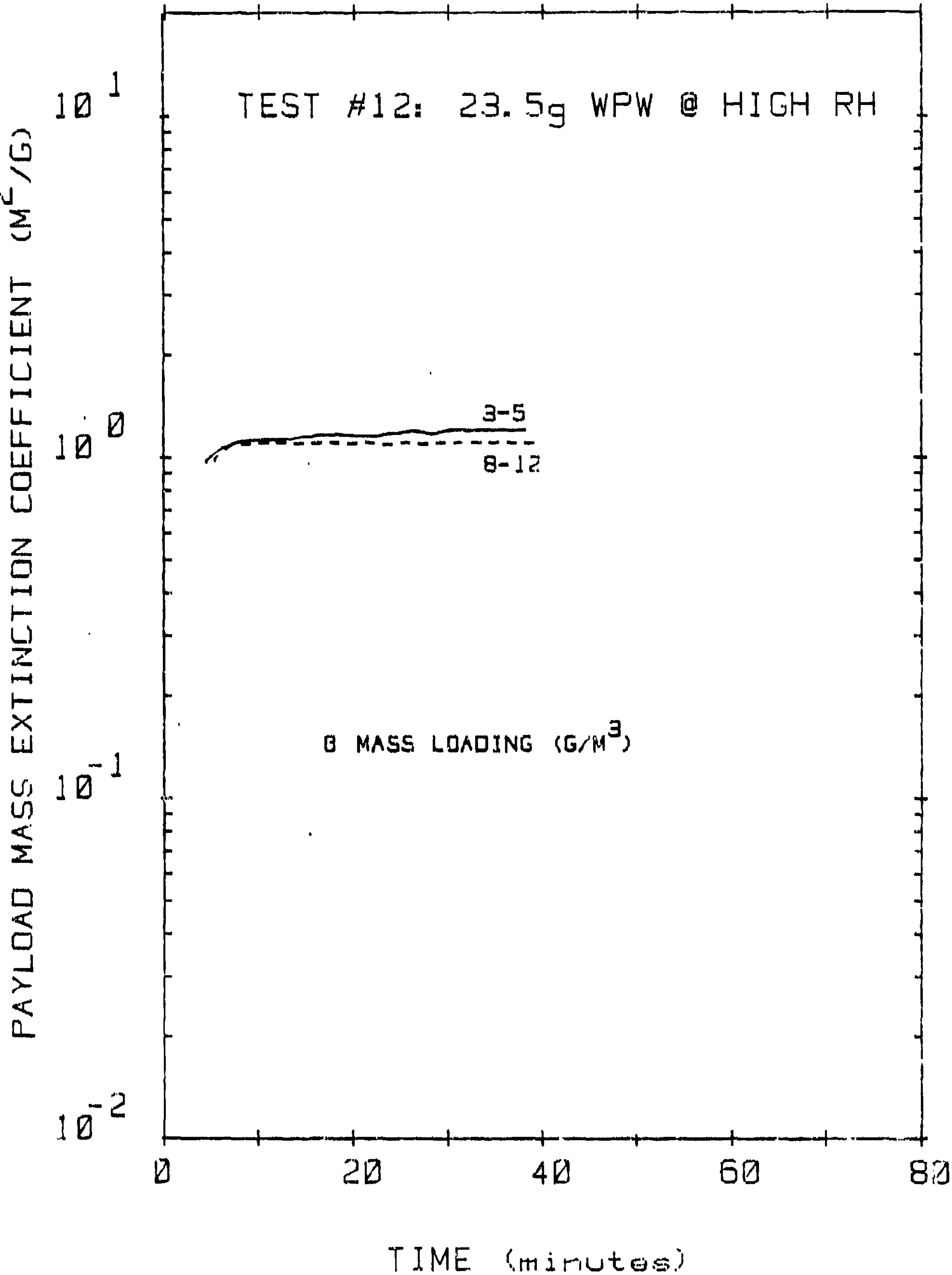

TEST #12: 23.5g WPW @ HIGH RH
PAYLOAD MASS EXTINCTION COEFFICIENT (M2/G)
10 1
10 0
10 -1
10 -2
3-5
8-12
B MASS LOADING (G/M3)
0
20
40
60
80
TIME (minutes)

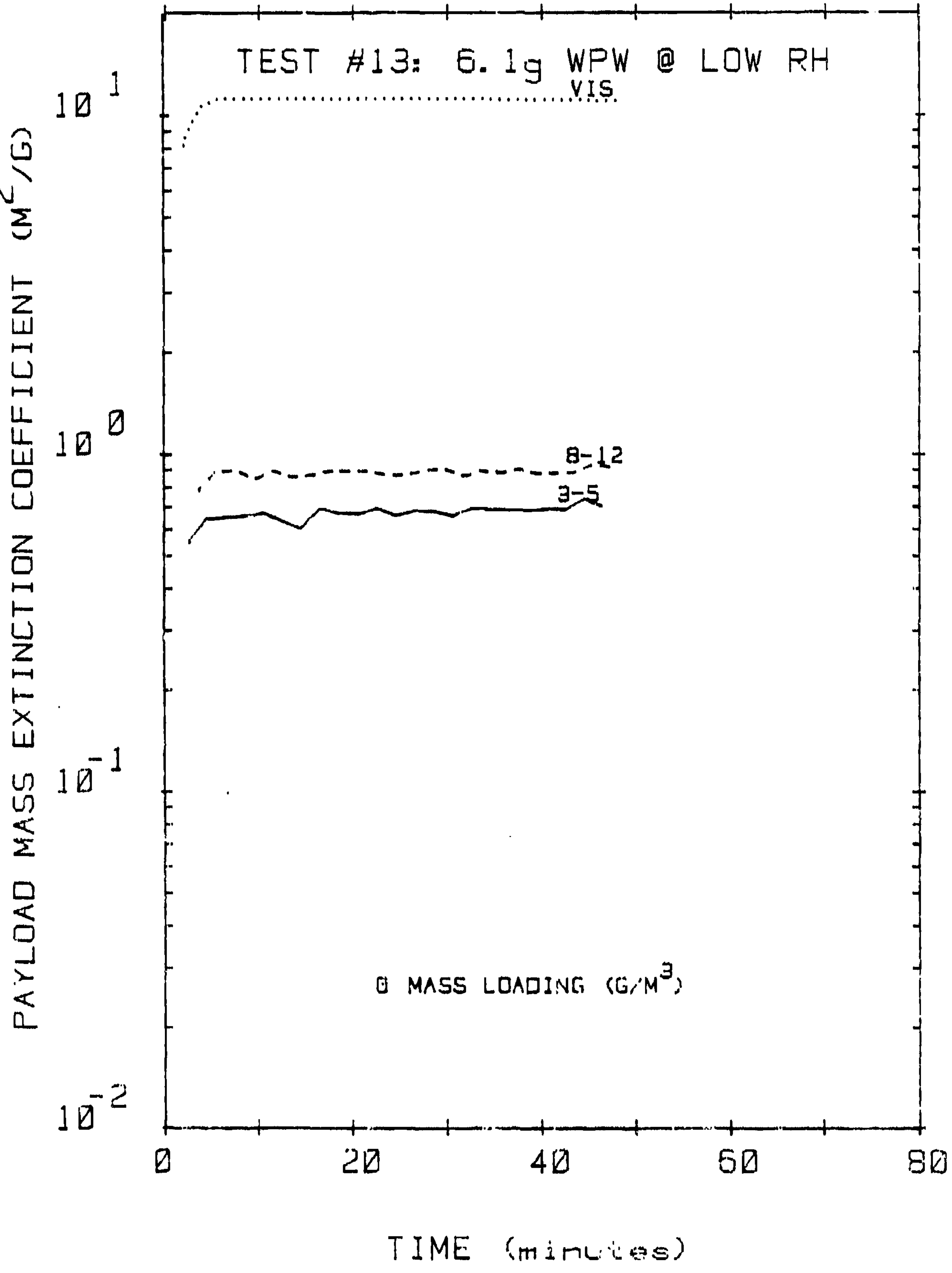
TEST #13: 6.1g WPW @ LOW RH
VIS
8-12
3-5
0 MASS LOADING (G/M^3)
PAYLOAD MASS EXTINCTION COEFFICIENT (M^2/G)
10^1
10^0
10^-1
10^-2
0
20
40
60
80
TIME (minutes)